

Diagnostic Software System for Automated Classification of Lung Sounds Based on Higher-Order Spectra Parameters

Porieva H. S.¹, Ivanko K. O.¹, Karpliuk Ye. S.¹, Popov A. O.¹, Philip de Chazal²

¹National Technical University of Ukraine “Ihor Sikorsky Kyiv Polytechnic Institute”, Kyiv, Ukraine

²Charles Perkins Centre, Faculty of Medicine and Health, University of Sydney, Sydney, Australia

E-mail: porevanna-ee@lil.kpi.ua, ivanko-ee@lil.kpi.ua, yk-ee@lil.kpi.ua, popov-ee@lil.kpi.ua, philip.dechazal@sydney.edu.au

This paper presents a method for the automated classification of lung sounds based on Higher-Order Spectra (HOS) parameters. The system is designed to differentiate between healthy subjects and patients with bronchitis or Chronic Obstructive Pulmonary Disease (COPD). The study was conducted using a verified database of 806 recordings from 275 adult patients, obtained via the “KoRA-03M1” digital system, the Littmann 3200 stethoscope, and the open international ICBHI 2017 Respiratory Sound Database (Kaggle). Particular attention is paid to the signal preprocessing stage, which includes an algorithm for removing impulse noise (“spikes”) present in the recorded signals using a bidirectional filtering method. Unlike traditional linear analysis methods, the proposed HOS-based approach accounts for the nonlinear properties of signals and identifies hidden phase coupling between harmonics, which is critical for analyzing noisy biomedical data. Seven optimal features providing maximum class separability were used: the amplitudes of dominant bispectrum peaks, the coordinates of their corresponding bifrequencies, maximum bicoherence, and third- and fourth-order statistical moments (skewness and kurtosis). Based on the compiled database, machine learning models were trained. Multilayer Perceptron (MLP) neural networks demonstrated the highest performance, achieving an accuracy of 97.8%. The results confirm the high diagnostic value of using bispectrum parameters as reliable markers of respiratory pathologies, supporting the integration of the developed software system into modern telemedicine systems for remote monitoring.

Keywords: lung sounds; Higher-Order Spectra; bispectral analysis; automated classification; machine learning; chronic obstructive pulmonary disease; bronchitis

DOI: [10.64915/RADAP.2026.104.54-62](https://doi.org/10.64915/RADAP.2026.104.54-62)

Introduction

Automated analysis of lung sounds is one of the most promising areas of modern biomedical engineering, as it allows for the elimination of the subjectivity inherent in traditional auscultation and provides a quantitative assessment of pathological respiratory sounds. The reliability of classical auscultation significantly depends on the physician’s experience, examination conditions, and individual hearing sensitivity, which creates difficulties in the early diagnosis of bronchitis, Chronic Obstructive Pulmonary Disease (COPD), and other diffuse disorders of the respiratory system.

The development of digital stethoscopes and machine learning methods has contributed to the rapid proliferation of lung sound analysis systems. Such systems most frequently utilize time-frequency features: spectrograms, mel-spectrograms, Mel-Frequency Cepstrum Coefficients (MFCC), and Gammatone Cepstral Coefficients (GTCC). Due to

their stability and integration with deep convolutional networks, these representations provide classification accuracy ranging from 85–95% [1–4]. Hybrid architectures, combining Convolutional Neural Networks (CNN) with Long Short-Term Memory (LSTM) or Gated Recurrent Units (GRU), improve generalization across various recording conditions and provide higher robustness despite significant patient and sensor variability [5, 6]. Hardware-aware models optimized for portable devices allow such systems to be implemented in telemedicine solutions and remote monitoring [7].

Despite significant progress, the vast majority of modern algorithms are based on linear features that reflect the power spectrum but largely overlook the nonlinear nature of pathological lung sounds. The physical basis for such non-linearity lies in the complex mechanisms of lung sound generation. During respiration, the airflow through the branching bronchial tree transitions from laminar to turbulent, causing nonlinear vibrations of the airway walls and intermittent airway opening and closing. These processes

generate acoustic signals that contain phase-coupled harmonics, which cannot be fully characterized by linear power spectra but are effectively captured by Higher-Order Spectra (HOS) analysis. Under these conditions, spectral and mel-spectral representations may lose subtle but vital patterns, thereby limiting diagnostic sensitivity [8, 9].

In this regard, there is growing interest in methods capable of describing nonlinear signal properties. There are at least three reasons for using HOS in biomedical signal processing, which allow for the analysis of phase coupling between harmonics and nonlinear component interactions. First, HOS do not contain Gaussian noise components, making it possible and more straightforward to detect useful signals, estimate key parameters, and even reconstruct weak, noisy signals. Second, unlike the power spectrum, HOS retain signal phase information, enabling the detection of nonlinear phase coupling between spectral components. Third, since HOS are nonlinear functions of the data, they serve as a convenient tool for identifying and evaluating nonlinear relationships in biomedical signals – specifically, signal properties that manifest as sound distortions in various pathologies. Thus, these characteristics are resistant to additive noise and reflect deeper signal patterns that arise during pathological changes in the bronchial tree [10–12].

The HOS approach enables the use of informative indicators such as maximum bispectral amplitude, frequency coordinates of the bispectral peak, bispectrum areas in various frequency ranges, bispectral entropy, skewness, kurtosis, and integral energy characteristics. These parameters have demonstrated high sensitivity to ventilation disorders and changes in respiratory mechanics in pathologies such as bronchitis and COPD [13–15].

Certain aspects of lung sound analysis and the use of spectral and nonlinear parameters have been previously explored by the authors [16, 18]; however, the results of a comparative analysis for healthy individuals, patients with chronic bronchitis, and COPD, along with the implementation of the diagnostic software system, are published here for the first time.

Therefore, developing a system that integrates HOS analysis of lung sounds with machine learning methods to improve the differentiation accuracy between healthy individuals and patients with bronchitis or COPD is highly relevant. This approach has the potential to create interpretable, noise-resistant, and technically streamlined telemedicine solutions and portable diagnostic complexes.

1 Materials and Methods

1.1 Lung Sound Database

The study was conducted using a database of 806 breath sound recordings from 275 adult patients. For

the automated classification task, the data were organized into four distinct classes based on the clinical verification:

1. Healthy individuals (234 recordings);
2. Chronic bronchitis (168 recordings);
3. COPD with basal lower lobe pneumofibrosis (135 recordings);
4. COPD with diffuse pneumofibrosis (119 recordings).

A total of 143 patients were diagnosed with COPD; however, for classifier training, only recordings with a confirmed specific subtype (basal or diffuse) were utilized to ensure high labeling accuracy.

The respiratory status of the patients was verified by a pulmonologist based on standard clinical diagnostic methods, including auscultation, spirometry, and X-ray examination.

Most signals were obtained using the “KoRA-03M1” four-channel phonospirographic system with a sampling frequency of 3496 Hz. Lung sounds were recorded synchronously across four channels, with an average recording duration of 20 seconds. The simultaneous use of four channels allowed for the analysis of respiratory activity from different points on the patient’s chest. Piezoelectric accelerometer sensors were attached at four specific points selected according to pulmonological recommendations: typically, two sensors were placed on the anterior chest wall at the level of the 2nd rib along the midclavicular line, and two sensors were placed on the back at the level of the 7th rib near the inferior angle of the scapula [19].

A portion of the recordings was obtained using a Littmann 3200 digital stethoscope and from the open-access ICBHI 2017 Respiratory Sound Database (Kaggle), with a sampling frequency of 4000 Hz [20].

1.2 Signal Preprocessing

Prior to analysis, all signals underwent a preprocessing stage, which included filtration, normalization, removal of random impulse noise, and segmentation into respiratory phases.

A digital high-pass filter was used to eliminate frequency components below 80 Hz, as this range is dominated by physiological sounds unrelated to respiration, while informative lung sound content in this band is negligible. Furthermore, a narrowband notch filter suppressed frequency components around 150 Hz. This is necessary because power grid interference, often caused by pulsed loads, manifests as significant nonlinear distortions on odd harmonics.

Since the relative relationship to the Root Mean Square (RMS) value is more critical for this research than absolute amplitude, signal normalization was

performed to eliminate the influence of recording conditions:

$$\tilde{X}_i = \frac{X_i - \bar{X}}{\sqrt{\frac{1}{N} \sum_{i=1}^N (X_i - \bar{X})^2}}, \quad (1)$$

where \tilde{X}_i is the normalized signal, X_i is the original signal, \bar{X} is the average value of the original signal, and N is the number of samples.

Due to their high sensitivity, the sensors record extraneous ambient noise and artifacts caused by minor movements or the sensors sliding on the patient's body. These result in "spikes" that significantly complicate further analysis. Given the short impulse response of the input path, this work proposes a preprocessing method to eliminate these spikes.

The spike filtering procedure is performed as follows. First, a reference signal is constructed as the modulus of the derivative approximation of the filtered signal. Spikes are detected by thresholding this reference signal. For each detected spike, a processing window is defined and extended by a predefined number of samples. The signal within this window is then smoothed using either a moving average filter or bidirectional filtering (Fig. 1).

Figures 2 and 3 present lung signal plots across four channels: the original signal is shown in blue, red highlights the segments where the proposed method detected spikes, and green represents the sig-

nal smoothed after the applied filtering. Thus, the application of the method for detecting and removing random spikes significantly enhances the success of subsequent digital signal analysis aimed at identifying diagnostically valuable parameters by reducing the influence of random interference.

For a detailed analysis of the localization of pathological artifacts within the respiratory cycle, an algorithm for automated signal segmentation into inhalation and exhalation phases was applied. The method is based on the time-frequency analysis of the output signal, during which two frequency regions are identified on the spectrogram: the main respiratory activity band (200–500 Hz) and a reference band of non-stationary broadband noise (800–1200 Hz). To minimize the impact of parasitic noise bursts on the cycle detection process, an adaptive filtering procedure based on the LMS (Least Mean Squares) algorithm is utilized, where the synthesized noise signal serves as a reference for cleaning the respiratory activity signal.

The resulting digitized envelope profile undergoes additional low-pass filtering with a cutoff frequency of 4 Hz and is processed by a thresholding algorithm. This allows for the precise detection of respiratory phase boundaries and enables subsequent HOS analysis to be performed for each segment individually. This algorithm is described in greater detail in the authors' previous work [16].

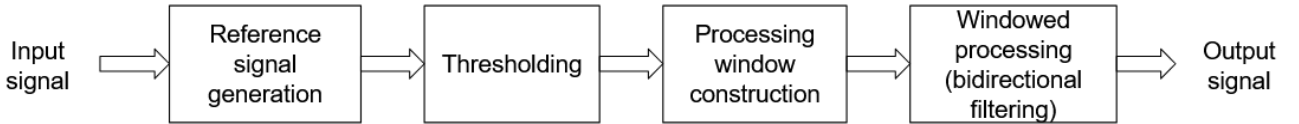


Fig. 1. Diagram illustrating the procedure for random spike removal.

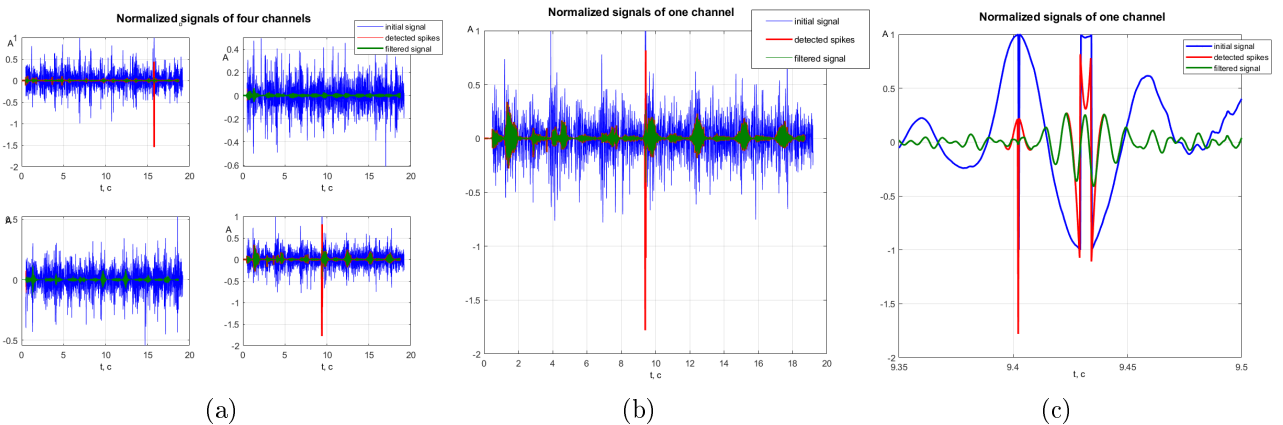


Fig. 2. (a) Four channels of the recorded respiratory sound signal: blue – original signal with spikes, red – detected spikes, green – signal after the proposed filtering algorithm; (b) 4th channel of the recorded signal; (c) enlarged fragment of the 4th channel signal.

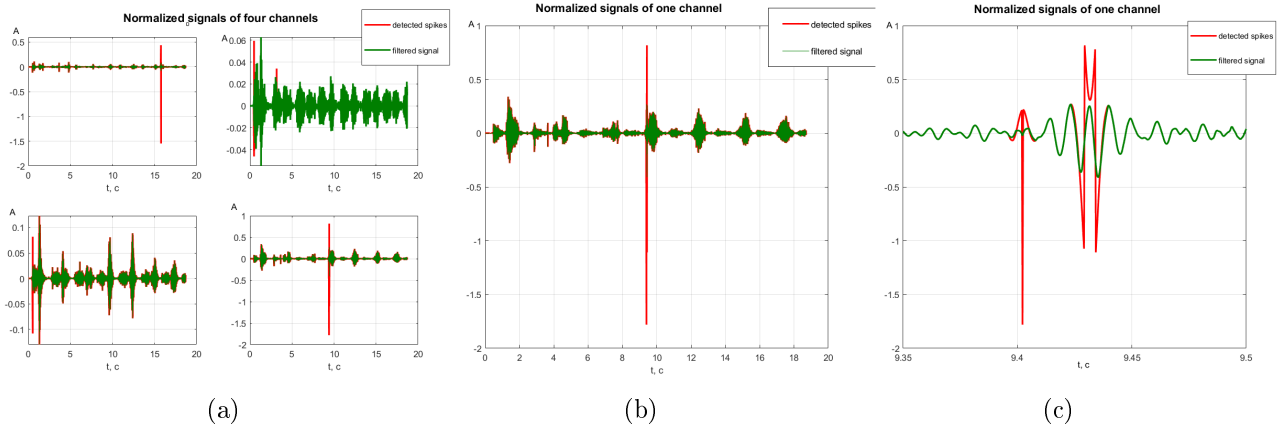


Fig. 3. (a) Four channels of the recorded respiratory sound signal: red – detected spikes, green – filtered signal after the applied algorithm; (b) 4th channel of the recorded signal; (c) enlarged fragment of the 4th channel signal.

1.3 Lung Sound Parameters Based on Higher-Order Spectra

The proposed method is based on the application of Higher-Order Spectra, specifically bispectral analysis, to identify diagnostically valuable parameters of lung sounds. HOS methods allow for the suppression of Gaussian noise, the preservation of signal phase information, and the detection of nonlinear interactions, which are essential for biomedical signal analysis.

1.3.1 Bispectrum

The bispectrum $B(f_1, f_2)$ is a two-dimensional Fourier transform of the third-order cumulant function $c_3(\tau_1, \tau_2)$. It was calculated using two approaches: the direct non-parametric method and the indirect cumulant-based method.

In the direct method, the bispectrum $B(k_1, k_2)$ is calculated by averaging the third-order spectrum over signal segments:

$$B(k_1, k_2) = \frac{1}{M} \sum_{i=1}^M F_{x_i}(k_1) F_{x_i}(k_2) F_{x_i}^*(k_1 + k_2), \quad (2)$$

where M is the number of segments into which the output signal $X(k)$ is divided; k_1 and k_2 are discrete frequency indices; $F_{x_i}(k)$ is the discrete Fourier transform of the i -th signal segment $x_i(n)$; and $F_{x_i}^*(k_1 + k_2)$ is the complex-conjugate value of the DFT for frequency $k_1 + k_2$.

The following parameters were used for analysis: V_1 , V_2 , and V_3 , which are the amplitudes of the three largest bispectral peaks ranked from maximum to minimum; and f_1 , f_2 , and f_3 , which are the normalized bifrequencies where these peaks are observed.

In the indirect method, the bispectrum $B(f_1, f_2)$ is calculated as a two-dimensional Fourier transform of

the mean third-order cumulants $c_3(\tau_1, \tau_2)$:

$$B(f_1, f_2) = \sum_{\tau_1=-\infty}^{\infty} \sum_{\tau_2=-\infty}^{\infty} c_3(\tau_1, \tau_2) \times e^{-j(\omega_1 \tau_1 + \omega_2 \tau_2)} w(\tau_1, \tau_2), \quad (3)$$

where $c_3(\tau_1, \tau_2)$ is the third-order cumulant function, $w(\tau_1, \tau_2)$ is a two-dimensional window used to smooth edge effects, and f_1, f_2 are normalized bifrequencies.

1.3.2 Parametric Bispectrum

The parametric bispectrum was calculated based on an autoregressive (AR) model, which enhances the detection of nonlinear signal properties:

$$S_3^X(\omega_1, \omega_2) = \beta H(\omega_1) H(\omega_2) H^*(\omega_1 + \omega_2), \quad (4)$$

where β is the third-order moment of the non-Gaussian stationary white noise in the AR model; $H(f)$ is the transfer function of the p -th order AR model; $H^*(f_1 + f_2)$ is the complex-conjugate transfer function at the frequency $f_1 + f_2$; and f_1, f_2 are normalized bifrequencies.

1.3.3 Bicoherence Function

The bicoherence function $\gamma_3(f_1, f_2)$ is a dimensionless normalized magnitude that measures the quadratic phase coupling between two frequency components. It is calculated using the bispectrum and the power spectrum:

$$\gamma_3(f_1, f_2) = \frac{|B(f_1, f_2)|^2}{P(f_1)P(f_2)P(f_1 + f_2)}, \quad (5)$$

where $|B(f_1, f_2)|^2$ is the squared magnitude of the bispectrum and $P(f)$ is the power spectrum at frequency f . A value of $\gamma_3(f_1, f_2) = 1$ indicates complete phase coupling due to nonlinearity, while a value of 0 indicates its absence. In this work, the maximum bicoherence $\gamma_{3\max}$ and its corresponding bifrequencies were analyzed as diagnostic features.

1.3.4 Skewness and Kurtosis Coefficients

These coefficients are used to estimate the degree of deviation of the observed process from a Gaussian distribution. Skewness was calculated as

$$c_3 = \frac{K_3}{\sigma^3}, \quad (6)$$

where K_3 is the third-order cumulant and σ is the standard deviation. Non-zero c_3 values allow for the assessment of the nature and extent of the signal's deviation from Gaussian noise. Kurtosis was calculated as

$$c_4 = \frac{K_4}{\sigma^4} - 3, \quad (7)$$

where K_4 is the fourth-order cumulant. The subtraction of 3 is performed because the kurtosis of a univariate normal distribution is 3. Thus, for a purely Gaussian process $c_4 = 0$.

The use of c_3 and c_4 in this study is justified by the need to quantify the non-Gaussianity of the signals, which serves as an important diagnostic marker for pathological processes. It was observed that while healthy lung sounds are statistically close to a Gaussian process, they remain non-Gaussian due to their non-stationary nature. The identification and analysis of these diagnostic features are further detailed in the authors' works [17, 18].

1.4 Automated Classification of Lung Sounds Based on HOS

Following the stages of signal preprocessing and the calculation of diagnostically significant HOS parameters, the automated classification of the bronchopulmonary system's state is implemented. The input for the classifiers is a feature vector formed from a selected set of HOS parameters that reflect the nonlinear properties and phase coupling of the signal's spectral components.

To optimize the classification model and ensure high generalization ability, a multi-stage feature selection process was implemented. First, a correlation analysis was conducted to reduce redundancy in the feature space. HOS parameters with a high mutual correlation coefficient ($|r| > 0.85$) were grouped, and only the most informative variable from each group was retained. Subsequently, the discriminative power of the remaining features was evaluated using the F-test. F-scores were used as the primary indicator of feature resolution, reflecting the extent to which the mean values of parameters differ across diagnostic groups relative to their intragroup variability.

Several classical machine learning algorithms that have proven effective in biomedical signal analysis with limited training datasets were investigated: Support Vector Machine with a radial basis function kernel, k -Nearest Neighbors, Logistic Regression, Naive Bayes, Classification and Regression Trees, and a Multilayer Perceptron feedforward neural network.

Model training and testing were conducted using the compiled database of lung sounds across four classes: healthy subjects, chronic bronchitis, and two subtypes of COPD. Feature normalization was applied to mitigate the impact of inter-individual variability and varying recording conditions. The database was partitioned into training (85%) and test (15%) sets using a patient-level split strategy. To ensure the objective evaluation of the model and prevent data leakage, all recordings belonging to the same individual were kept within the same subset. Furthermore, 7-fold cross-validation was conducted at the patient level, ensuring that the model was tested on data from subjects it had not encountered during the training phase.

Classification quality was evaluated using standard metrics: Precision, Recall, and F1-score:

$$P = \frac{TP}{TP + FP}, \quad (8)$$

$$Se = \frac{TP}{TP + FN}, \quad (9)$$

$$F1 = 2 \frac{P \cdot Se}{P + Se}, \quad (10)$$

where TP represents true positive, FP false positive, and FN false negative results. For the multiclass classification task, the final performance metrics were calculated using macro-averaging.

1.5 Structure of the Software Diagnostic System

The developed software diagnostic system consists of three main stages: preprocessing, analysis, and classification. The preprocessing stage includes filtering, normalization, spike removal, and segmentation into respiratory phases. The analysis stage includes calculation of diagnostically valuable parameters based on HOS. The classification stage provides automated decision-making regarding the state of the bronchopulmonary system. The structural diagram of the software diagnostic system is shown in Fig. 4.

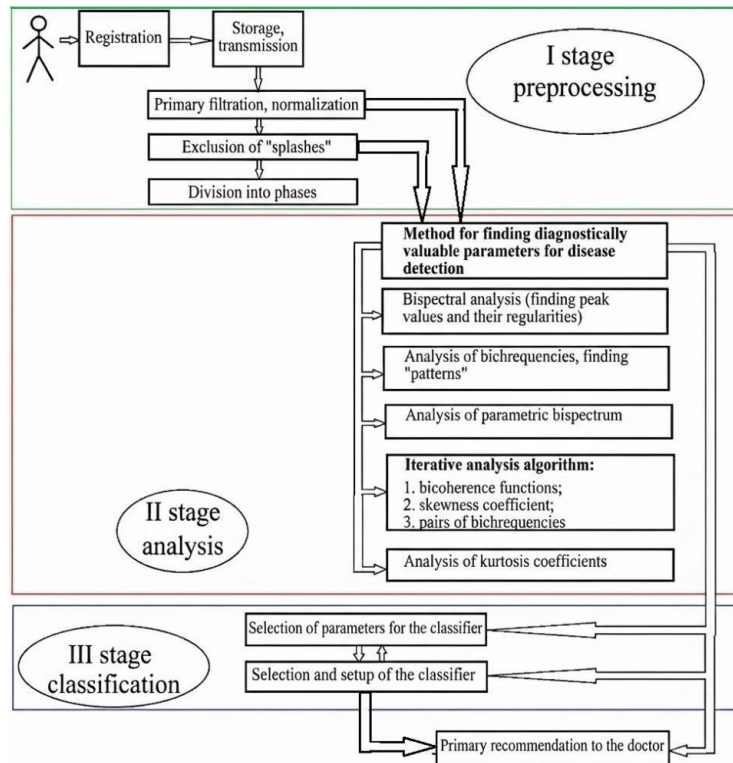


Fig. 4. Structural diagram of the software diagnostic system.

2 Results and Discussion

Based on the feature selection methodology described above, the analysis identified seven optimal parameters providing maximum class separability. The highest F-scores were achieved for the magnitudes of the first, second, and third largest peaks of the bispectrum (V_1 , V_2 , and V_3), their corresponding bifrequency coordinates, the skewness coefficient c_3 , the kurtosis coefficient c_4 , and the bifrequencies of the parametric bispectrum.

Numerical values of these seven optimal parameters were calculated for the entire database. To assess the discriminative power of the selected features across the diagnostic groups, a statistical analysis was performed. Instead of providing raw data for individual subjects, the distributions of these parameters are presented using box plots (Figs. 5–9). These visualizations represent the median, quartiles, and range for the total sample of 806 recordings, ensuring a comprehensive overview of the identified patterns without selection bias.

The analysis of the diagonal slice of the bispectrum revealed a set of amplitude peaks, which were ordered in descending order of their magnitude. Although the five largest peaks were analyzed to study the signal structure in detail, the coordinates of the first two peaks by amplitude demonstrated the greatest diagnostic significance: V_1 and V_2 .

Based on these data, a series of boxplots was constructed to compare the frequency coordinates of these peaks. Fig. 5 shows the comparative diagrams of the first and second normalized bifrequencies

corresponding to the first and second largest bispectral peaks for healthy individuals, patients with COPD, and patients with chronic bronchitis.

For healthy individuals, a clear pattern is observed: the value of bifrequency f_2 in the range from 0.035 to 0.06, which corresponds to the second peak, significantly exceeds the value of f_1 (0.028–0.035), corresponding to the maximum peak. In contrast, an inverse trend was found for patients with chronic bronchitis: the values of f_1 in the range from 0.03 to 0.05 exceed the values of f_2 (0.015–0.04). For patients with COPD, the bifrequencies f_1 and f_2 span a much wider range and show minimal differentiation, reflecting the complex and variable nature of pathological changes associated with this disease.

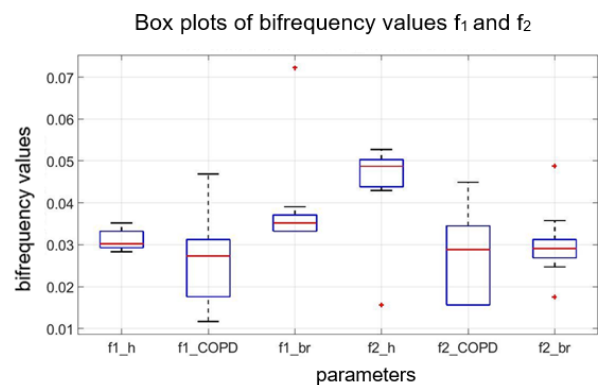


Fig. 5. Box plots of bifrequency values f_1 and f_2 for healthy individuals and patients with COPD and bronchitis.

Comparative data for the values of V_1 , V_2 , and V_3 are shown in Figs. 6 and 7. It was found that for healthy individuals, the parameter V_1 varies from 0.001 to 0.02, while V_2 is significantly smaller, ranging from 0.0004 to 0.003. For signals from patients with bronchitis, the V_1 parameter is smaller than that of a healthy person, whereas V_2 is larger. The same pattern is observed for the V_3 parameter.

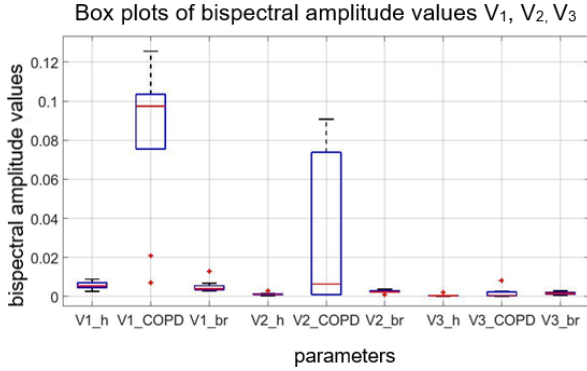


Fig. 6. Box plots of bispectral amplitude values V_1 , V_2 , and V_3 for healthy individuals and patients with COPD and bronchitis.

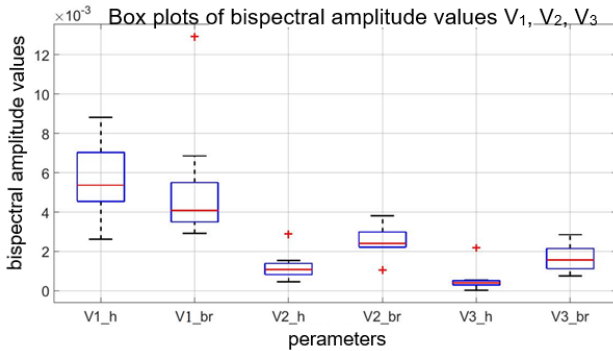


Fig. 7. Box plots of bispectral amplitude values V_1 , V_2 , and V_3 for healthy individuals and patients with bronchitis.

For patients with COPD, it was found that the bispectral peak amplitudes are significantly larger than those of healthy individuals. For instance, while V_1 for healthy subjects lies between 0.002 and 0.01, for COPD patients this value fluctuates around the 0.08–0.1 range. The parameters V_2 and V_3 in COPD patients are also larger than the corresponding values in both healthy individuals and patients with bronchitis.

The skewness c_3 for healthy subjects remains within ± 0.15 , with the mean signal value close to zero, indicating a symmetrical amplitude distribution characteristic of a normal distribution. In pathologies, a significant deviation from zero and distribution asymmetry are observed (Fig. 8). For healthy individuals, the kurtosis c_4 fluctuates around 3, consistent with the Gaussian distribution. Conversely, in COPD, c_4 values can exceed those of healthy individuals by one

or two orders of magnitude, indicating a sharp peak caused by intense pathological spikes (Fig. 9).

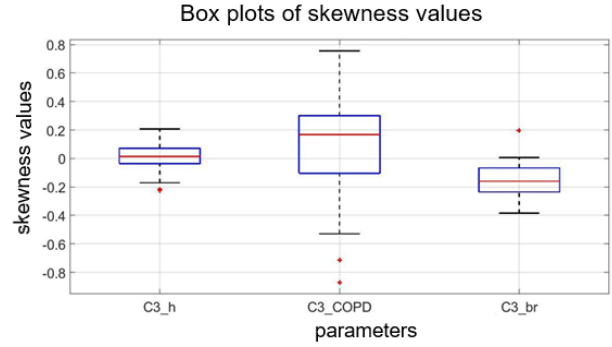


Fig. 8. Box plots of skewness values for healthy individuals, patients with COPD, and patients with bronchitis.

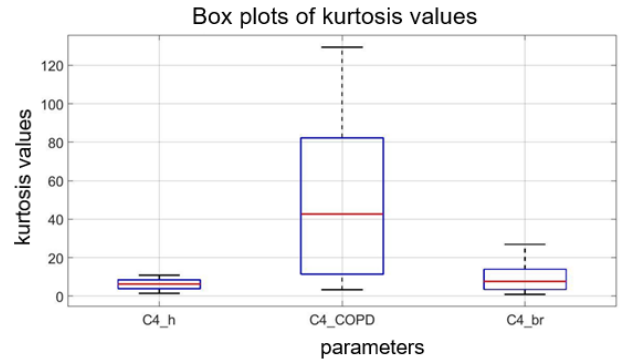


Fig. 9. Box plots of kurtosis values for healthy individuals, patients with COPD, and patients with bronchitis.

Since theoretically, Higher-Order Spectra for purely Gaussian processes are zero, the detection of non-zero HOS parameters allows for the effective extraction of informative pathological features against the background of physiological respiratory noise.

For comparison, Table 1 presents the peak coordinates (f_1, f_2) on the parametric bispectrum plane for the three study groups.

The frequency pair determines the position of the maximum nonlinear response. It was established that for patients with bronchitis, the values of the first and second bifrequencies of a single peak practically coincide ($f_1 \approx f_2$). This indicates that the dominant maximum is located on the diagonal of the bispectral surface, suggesting an intensive nonlinear interaction between a frequency and its own second harmonic.

Such comparative graphs and tables can be provided for all identified diagnostically significant parameters. However, the adequate comparison and analysis of a large number of such parameters requires specific expertise and training. It should be noted that the results were obtained on a verified but limited sample, which underscores the necessity for further external validation of the proposed approach using independent databases.

Table 1 Parametric bispectrum bifrequency values (f_1, f_2) for the three study groups

Healthy		COPD		Bronchitis	
f_1	f_2	f_1	f_2	f_1	f_2
0.02734375	0	0.05175781	0.050257	0.0361328	0.0361328
0.02930	0	0.0283203	0	0.035156	0.035156
0.05859375	0.03710937	0.017578	9.7656×10^{-4}	0	0
0.03320312	0	0.015625	0.01362	0.0380859	0.0380859
0.03417968	0.03222656	0.0341796	0	0.03710937	0.03710937

Based on the selected feature set, machine learning classifiers were trained and evaluated. Comparative analysis demonstrated that HOS parameters provide consistently high performance across all studied classes. The best generalization ability was achieved by the decision tree and the multilayer neural network.

An analysis of the category-wise classification results obtained with the Multilayer Perceptron (MLP) neural network, which achieved the highest overall accuracy of 97.8%, revealed notable differences in recognition quality. The highest reliability was observed for the “Healthy” class (precision 99%, recall 98%, F1-score 98.5%) and “COPD with diffuse pneumofibrosis” (precision 98%, recall 99%, F1-score 98.5%). This confirms that for these conditions, HOS parameters form the most distinct and stable diagnostic patterns. The “Chronic bronchitis” category was recognized with 96% precision and 95% recall, representing a significant improvement over linear features such as MFCC, where this class is frequently misclassified as normal. The most challenging category to identify was “COPD with basal lower lobe pneumofibrosis”. While its precision remained high at 98%, its recall was lower at 89%.

Despite the high overall average accuracy, the system is most effective at differentiating healthy states from diffuse lung lesions, whereas localized forms of COPD require more rigorous feature analysis. These results align with the authors’ previous findings regarding the efficacy of combining nonlinear features with machine learning for lung sound analysis [17, 18]. However, in this study, the classification stage is presented as an integral component of a comprehensive software diagnostic system designed for practical clinical application.

Experimental studies established that using HOS features allows the Decision Tree model to achieve an accuracy of 96.2% with a specificity of 96.5%. The best performance was demonstrated by the MLP neural network, which showed an accuracy of 97.8%, sensitivity of 96.8%, and specificity of 97.4%. For comparison, using only MFCC on the same dataset yielded an accuracy no higher than 89.3%, which confirms the advantage of incorporating nonlinear features.

Conclusions

This paper presents an approach for the automated analysis and classification of lung sounds based on

Higher-Order Spectra parameters. Unlike traditional spectral and mel-cepstral features, the proposed approach effectively describes nonlinear, phase-coupled, and non-stationary interactions between signal components. These interactions are characteristic of the respiratory sound generation processes during pathological changes in the bronchopulmonary system.

Within the scope of this study, several bispectral and statistical parameters were analyzed, including bispectral amplitude characteristics, their corresponding bifrequencies, integral energy indicators, skewness, kurtosis, and bispectral entropy. It was demonstrated that these features are highly sensitive to pathological changes in respiratory mechanics and show statistically significant differences between healthy individuals, patients with chronic bronchitis, and patients with COPD.

The application of correlation analysis and the F-test facilitated the selection of an optimal set of HOS parameters, providing a balance between diagnostic informativeness and computational complexity. The resulting compact feature space is robust against additive noise and suitable for implementation in automated decision support systems.

The effectiveness of this approach was confirmed by machine learning results, where the inclusion of HOS features ensured high-quality differentiation between the studied groups, significantly outperforming results obtained using only linear spectral characteristics.

The developed software diagnostic system implements the full signal processing cycle, from preprocessing and spike removal to the visualization of classification results. The modular architecture of the system allows for adaptation to various recording conditions and serves as a foundation for developing portable and telemedicine screening systems for respiratory diseases.

Future research directions include expanding the database to validate the method on larger patient cohorts; investigating the effectiveness of the approach for other respiratory pathologies such as asthma, pneumonia, and interstitial lung diseases; and integrating HOS features with time-frequency representations within hybrid deep learning architectures to further enhance diagnostic reliability.

References

- [1] T. Wanasinghe, S. Bandara, S. Madusanka, D. Meedeniya, M. Bandara, and I. D. L. T. Diez. (2024). Lung sound classification with multi-feature integration utilizing lightweight CNN model. *IEEE Access*, Vol. 12, pp. 21262-21276. DOI: 10.1109/ACCESS.2024.3361943.
- [2] Y. Zhang, Q. Huang, W. Sun, F. Chen, D. Lin, and F. Chen. (2024). Research on lung sound classification model based on dual-channel CNN-LSTM algorithm. *Biomed. Signal Process. Control*, Vol. 94, Art. no. 106257. DOI: 10.1016/j.bspc.2024.106257.
- [3] D.-M. Huang, J. Huang, K. Qiao, N.-S. Zhong, H.-Z. Lu, and W.-J. Wang. (2023). Deep learning-based lung sound analysis for intelligent stethoscope. *Mil. Med. Res.*, Vol. 10, No. 1, Art. no. 44. DOI: 10.1186/s40779-023-00479-3.
- [4] G. Altan, Y. Kutlu, and N. Allahverdi. (2020). Deep learning on computerized analysis of chronic obstructive pulmonary disease. *IEEE J. Biomed. Health Inform.*, Vol. 24, No. 5, pp. 1344-1350. DOI: 10.1109/JBHI.2019.2931395.
- [5] Lweesy K., Abuqran S., Fraiwan L. (2025). Lightweight Hybrid Deep Learning Models for Accurate Classification of Respiratory Conditions from Raw Lung Sounds. *J Med Syst.*, 49(1):174. doi: 10.1007/s10916-025-02315-8. PMID: 41315171.
- [6] G. Petmezas, G.-A. Cheimariotis, L. Stefanopoulos, B. Rocha, R. P. Paiva, et al. (2022). Automated lung sound classification using a hybrid CNN-LSTM network and focal loss function. *Sensors*, Vol. 22, No. 3, Art. no. 1232. DOI: 10.3390/s22031232.
- [7] X. Liao, Y. Wu, N. Jiang, et al. (2023). Automated detection of abnormal respiratory sound from electronic stethoscope and mobile phone using MobileNetV2. *Biocybernetics and Biomedical Engineering*, Vol. 43, Iss. 4, pp. 63-775, ISSN 0208-5216, doi:10.1016/j.bbe.2023.11.001.
- [8] K.-C. Chua, V. Chandran, U. R. Acharya, and C. M. Lim. (2010). Application of higher order statistics/spectra in biomedical signals — A review. *Med. Eng. Phys.*, Vol. 32, No. 7, pp. 679-689. DOI: 10.1016/j.medengphy.2010.04.009.
- [9] R. Dubey, R. M. Bodade, and D. Dubey. (2023). Efficient classification of the adventitious sounds of the lung through a combination of SVM-LSTM-Bayesian optimization algorithm with features based on wavelet bi-phase and bi-spectrum. *Res. Biomed. Eng.*, Vol. 39, pp. 349-363. DOI: 10.1007/s42600-023-00270-2.
- [10] R. Palaniappan, K. Sundaraj, and S. Sundaraj. (2014). A comparative study of the SVM and k-NN machine learning algorithms for the diagnosis of respiratory pathologies using pulmonary acoustic signals. *BMC Bioinformatics*, Vol. 15, No. 1, Art. no. 223. DOI: 10.1186/1471-2105-15-223.
- [11] A. M. Kwon and K. Kang. (2022). A temporal dependency feature in lower dimension for lung sound signal classification. *Sci. Rep.*, Vol. 12, Art. no. 7889. DOI: 10.1038/s41598-022-11726-3.
- [12] S. B. Sangle and C. J. Gaikwad. (2023). Accumulated bispectral image-based respiratory sound signal classification using deep learning. *Signal, Image and Video Processing*, Vol. 17, pp. 3629-3636. DOI: 10.1007/s11760-023-02589-w.
- [13] A. Rao, E. Huynh, T. J. Royston, A. Kornblith, and S. Roy. (2019). Acoustic Methods for Pulmonary Diagnosis. *IEEE Rev. Biomed. Eng.*, Vol. 12, pp. 221-239. DOI: 10.1109/RBME.2018.2874353.
- [14] Garcia-Mendez, Juan P., et al. (2023). Machine Learning for Automated Classification of Abnormal Lung Sounds Obtained from Public Databases: A Systematic Review. *Bioengineering*, Vol. 10, No. 10: 1155. DOI: 10.3390/biengineering10101155.
- [15] L. Fraiwan, N. Hassanin, M. Fraiwan, B. Khassawneh, A. E. Ibnian, and M. Alkhodari. (2021). Automatic identification of respiratory diseases from stethoscopic lung sound signals using ensemble classifiers. *Biocybern. Biomed. Eng.*, Vol. 41, No. 1, pp. 1-14. DOI: 10.1016/j.bbe.2020.11.003.
- [16] H. S. Porieva, Y. S. Karplyuk, A. Makarenkova, and A. Makarenkov. (2015). Detection of COPD's diagnostic signs based on polyspectral lung sounds analysis of respiratory phases. *ELNANO*, pp. 351-355. DOI: 10.1109/ELNANO.2015.7146908.
- [17] H. Porieva, B. Kaliuga and K. Ivanko. (2022). Differentiating of Respiratory Noise Based on Higher Order Spectral Analysis. *ELNANO*, pp. 446-450. DOI: 10.1109/ELNANO54667.2022.9927121.
- [18] H. S. Porieva, V. I. Vaityshyn, and Y. S. Karplyuk. (2017). Machine learning methods for studying lungsound signals. *Microsyst. Electron. Acoust.*, Vol. 22, No. 6, pp. 41-47. DOI: 10.20535/2523-4455.2017.22.6.108829.
- [19] A. A. Makarenkova. (2010). Investigation and objectifying of adventitious breath sounds in the patients with chronic obstructive pulmonary disease. *Acoust. Bull.*, Vol. 13, No. 3, pp. 31-41.
- [20] Respiratory Sound Database. *ICBHI 2017 Challenge, Kaggle*. [Online].

Діагностична програмна система для автоматизованої класифікації звуків легень на основі параметрів спектрів вищих порядків

Порева Г. С., Іванько К. О., Карплюк Є. С., Попов А. О., Філіп де Шазаль

У роботі представлено метод автоматизованої класифікації звуків легень на основі параметрів спектрів вищих порядків (Higher-Order Spectra, HOS). Система розроблена для диференціації станів здорових осіб та пацієнтів із бронхітом або хронічним обструктивним захворюванням легень (ХОЗЛ). Дослідження проведено з використанням верифікованої бази даних, що містить 806 записів від 275 дорослих пацієнтів, отриманих за допомогою цифрового комплексу «КоРА-03М1», стетоскопа Littmann 3200 та відкритого міжнародного набору даних ICBHI 2017 Respiratory Sound Database (Kaggle). Особливу увагу приділено етапу попередньої обробки сигналів, що включає оригінальний алгоритм видалення імпульсних завад («спайків») методом двонаправленої фільтрації. Використано сім оптимальних ознак, що забезпечують максимальну роздільну здатність класів. Найвищу ефективність продемонстрували нейронні мережі типу Multilayer Perceptron (MLP), досягнувши точності 97,8%. Отримані результати підтверджують діагностичну цінність параметрів біспектра як маркерів респіраторних патологій.

Ключові слова: звуки легень; спектри вищих порядків; біспектральний аналіз; автоматизована класифікація; машинне навчання; хронічне обструктивне захворювання легень; бронхіт